Bridge to Loop Transition in a Shear Aligned Lamellae Forming Heptablock Copolymer

Lifeng Wu,[†] Timothy P. Lodge,*[,†,‡] and Frank S. Bates*[,†]

Department of Chemical Engineering and Materials Science and Department of Chemistry, University of Minnesota, Minneapolis, Minnesota 55455

Received July 6, 2004
Revised Manuscript Received September 21, 2004

One of the most distinctive attributes of block copolymers is a propensity for certain morphologies to align in response to flow or deformation. This property was first documented by Keller and co-workers with cylinder-forming poly(styrene-*b*-butadiene-*b*-styrene) (SBS) triblock copolymer melts using extrusion, leading to mechanically anisotropic materials.[1] More than three decades of research have produced a litany of experimental findings that demonstrate phenomenological relationships among molecular parameters, such as chain architecture, composition, and segregation strength, and various processing variables including flow geometry (e.g., simple shear vs extrusion), shear rate, strain amplitude, and processing history.[2−29] Lamellae are especially intriguing as this morphology often displays two distinct and easily identified states of orientation (Figure 1) when subjected to shearing flows: the "parallel" arrangement with the layer normal directed perpendicular to the plane of shear, and the "perpendicular" form where the layers are organized perpendicular to the plane of shear with the layer normal coincident with the vorticity direction. (The third orthogonal arrangement, known as the "transverse" orientation, has been realized by abrupt cessation of shearing in certain pentablock copolymers[5] and by solution extrusion under some conditions.[30]) A rich literature documents the conditions leading to lamellae alignment and transitions between states of orientation, along with several theoretical concepts. Largely (but not totally[31]) absent from this discussion is a coherent connection between the collective microdomain (e.g., lamellae) response to flow and the underlying conformational state of individual block copolymer chains. Nevertheless, bridging and looping of internal blocks in multiblock copolymer melts have been implicated in flow-induced alignment of lamellae in triblock[30] and pentablock copolymers[5,6] and the resulting fracture properties in the solid state.[7,32] Figure 1 shows the two extremes of a fully bridged and a fully looped conformation, in the perpendicular and parallel orientations, respectively, to facilitate the subsequent discussion.

We have recently prepared a series of linear, compositionally symmetric, multiblock copolymers, ranging from poly(styrene-*b*-isoprene) (SI) diblock to SISISISISIS undecablock copolymers, for the purpose of exploring the influence of molecular architecture on the thermodynamics and dynamics of ordered lamellae.[33] Here we describe the response to oscillatory shear of a nearly

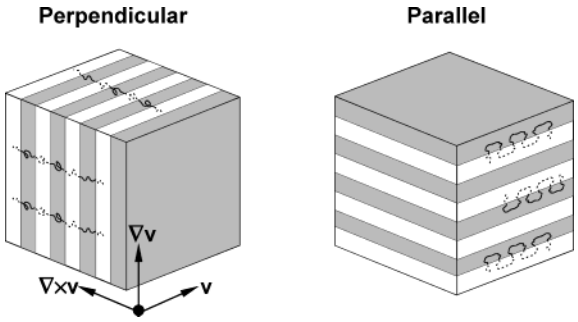

Figure 1. Coordinate system for reciprocating shear and states of lamellae alignment. Idealized heptablock copolymer molecular conformations, deduced from solvent swelling experiments, are identified within each morphology. The perpendicular orientation contains predominantly bridged chains, whereas the block copolymer is much more likely to loop along the interfaces in the parallel arrangement.

symmetric, lamellae-forming SISISIS heptablock copolymer. This polymer was prepared by sequential anionic polymerization of styrene and isoprene leading to a living SIS^-,Li^+ tetrablock that was coupled with α,α′-dibromo-*p*-xylene; size exclusion chromatography (SEC) analysis indicated a coupling efficiency of 94%. The overall number-average molecular weight of this polymer is $M_n = 1.04 \times 10^5$ g mol^{-1}, with polydispersity index $M_w/M_n < 1.07$. An overall S volume fraction of $f_S = 0.52$ (calculated from the molar composition established by ^{1}H NMR, using densities $\rho_S = 1.04$ g cm^{-1} and $\rho_I = 0.913$ g cm^{-1}) was achieved by making the S end blocks half the size of the internal S and I blocks. It should be noted that in several previous studies of multiblock $(SI)_n$ copolymers the end S blocks had the same length as the internal S blocks, leading to a total composition and domain spacing that depended significantly on n.[34−39] 0.5 wt % BHT antioxidant was added to the heptablock copolymer prior to sample preparation and testing.

Shear alignment was accomplished using a Rheometrics Scientific ARES rheometer containing a cone-and-plate fixture (25 mm diameter and 0.04 rad cone angle). Samples were compression-molded at 140 °C and then loaded into the instrument and heated to 201 °C, 10 deg above the order−disorder transition temperature (T_{ODT} = 191 °C). After 10 min, the rheometer tool was rapidly cooled to about 170 °C (this took about 3 min) and held at this temperature for 10 min. This procedure produces a finely dispersed arrangement (i.e., a "powder") of randomly oriented ordered domains.[33] Large-amplitude oscillatory shear was then applied until the magnitude of the recorded complex modulus, G^*, achieved a steady value. In a subsequent paper we intend to report on a comprehensive investigation of the flow aligning behavior of various multiblock copolymers, over a wide range of frequencies and strain amplitudes. This communication focuses on just two processing experiments carried out at 170 °C: strain amplitude $\gamma = 6$ and shear frequency $\omega = 0.02$ rad s^{-1} (sheared for 2 h) and $\gamma = 1$ and $\omega = 0.5$ rad s^{-1} (sheared for 1 h). After processing, the samples were cooled and carefully removed from the rheometer tool for structural analysis.

Small-angle X-ray scattering (SAXS) was employed to characterize the state of microdomain alignment in the sheared heptablock copolymer. Two-dimensional

[†] Department of Chemical Engineering and Materials Science.
[‡] Department of Chemistry.
* Authors for correspondence. E-mail: bates@cems.umn.edu, lodge@chem.umn.edu.

10.1021/ma048635w CCC: $27.50
Published on Web 10/01/2004

SAXS patterns were obtained using a lab-based instrument described elsewhere.[40] Scattering specimens, roughly 1 mm^3 in size, were cut from the center of the sheared plaques and mounted in three different ways, providing beam access to the shear (**v**), gradient (∇**v**), and vorticity ($\nabla\times$**v**) directions (see Figure 1). Scattering patterns were evaluated in two ways. First, integration over the azimuthal angle ϕ reduces the data to the one-dimensional form of intensity vs scattering wavevector, $q = |\mathbf{q}| = 4\pi\lambda^{-1}\sin(\theta/2)$. Narrow diffraction peaks located at q^*, $2q^*$, $3q^*$, ... signal a lamellar morphology with periodic spacing $D = 2\pi/q^*$ (data not shown).

Second, we have assessed lamellae orientation through the angular (ϕ) dependence of the scattering intensity at the principal peak wavevector q^* in each of the sample orientations, as illustrated in Figure 2. Distinctly different diffraction patterns are obtained for the two processing conditions. Two reflections in the $\mathbf{q}_{\nabla\mathbf{v}}-\mathbf{q}_{\nabla\times\mathbf{v}}$ and $\mathbf{q}_{\mathbf{v}}-\mathbf{q}_{\nabla\times\mathbf{v}}$ scattering planes, and absence of scattering in $\mathbf{q}_{\nabla\mathbf{v}}-\mathbf{q}_{\mathbf{v}}$, are consistent with a perpendicular arrangement of lamellae for the sample sheared at higher frequency and lower strain, while peaks in $\mathbf{q}_{\nabla\mathbf{v}}-\mathbf{q}_{\nabla\times\mathbf{v}}$ and $\mathbf{q}_{\nabla\mathbf{v}}-\mathbf{q}_{\mathbf{v}}$, rotated by 90°, and absence of diffraction in $\mathbf{q}_{\mathbf{v}}-\mathbf{q}_{\nabla\times\mathbf{v}}$ indicate a parallel orientation for the sample sheared at lower frequency and higher strain (see Figures 1 and 2). In both cases the degree of alignment is remarkably high. The spacing $D = 17.5$ nm for the perpendicular sample, 17.2 nm for the parallel sample, and 17.5 nm for the sample prior to shearing.

Transmission electron microscopy (TEM) was employed to provide real-space images of the shear-aligned specimens. Thin (ca. 75 nm) slices were cut at −100 °C using a Reichart Ultramicrotome equipped with a diamond knife, collected onto 400 mesh uncoated copper grids, and stained with the vapor from a 4% aqueous solution of osmium tetraoxide for 10 min. Figure 3 displays representative TEM images, taken on a JEOL 1210 instrument operating at 120 kV, from specimens subjected to each processing procedure. Both pictures reveal a high degree of alignment with nearly perfect translational order, consistent with the SAXS results found in Figure 2.

In a separate step, microtomed thin film specimens (supported on copper grids) were immersed in tetradecane for 1 h, followed by staining with osmium tetraoxide. The swollen films were then plunged into liquid nitrogen, mounted on a cryogenic sample holder (Gatan 626), and examined by TEM; representative images are presented in Figure 4. Exposure to tetradecane has no perceptible effect on the thin film derived from the perpendicular alignment (Figure 4a). However, the parallel film is influenced significantly by the solvent, exhibiting extensive buckling and delamination of the lamellae. Tetradecane is a good solvent for poly(isoprene) and a nonsolvent for poly(styrene), leading us to conclude that the parallel lamellae have delaminated through substantial swelling of the poly(isoprene) domains, whereas the perpendicular lamellae were highly resistant to swelling. Samples were reexamined by SEC after shearing and again after exposure to tetradecane; no detectable differences were observed.

Aside from a 90° rotation in space, and minor variations in the diffraction peak position and widths, the SAXS and TEM results (Figures 2 and 3) from the parallel and perpendicular lamellae specimens are essentially indistinguishable. Yet the swelling experiment summarized in Figure 4 leads to the inescapable conclusion that these two materials are fundamentally different at the microdomain level. We attribute this dramatic result to markedly different conformational states of the SISISIS heptablock copolymer in each orientation.

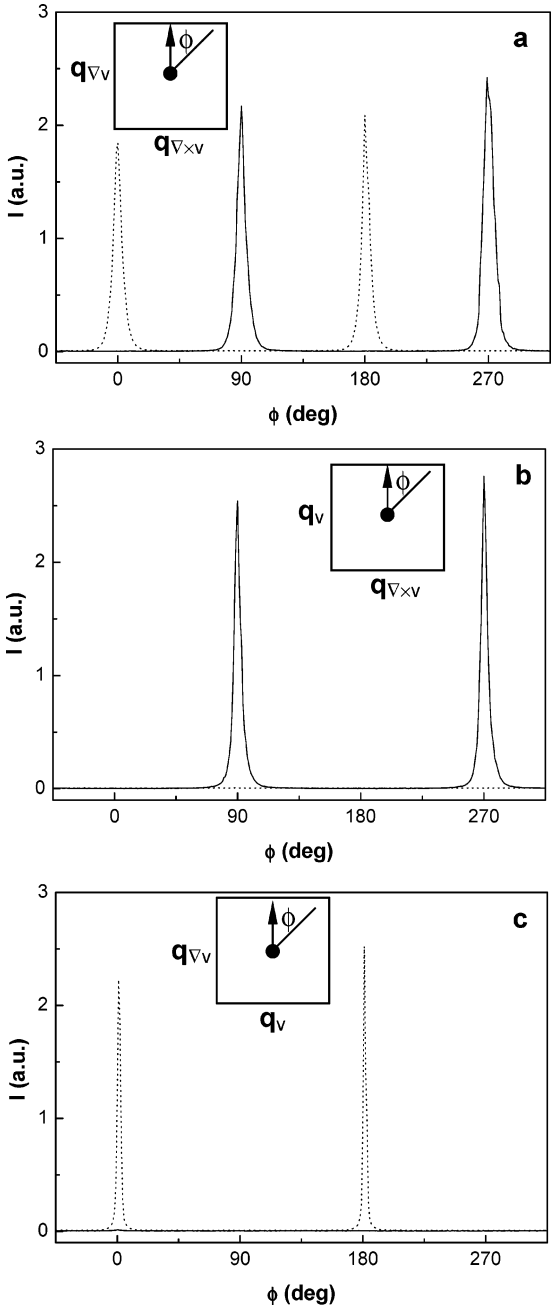

Figure 2. SAXS intensity at the principal wavevector q^* represented as a function of azimuthal angle ϕ, obtained with the X-ray beam directed along (a) shear direction (**v**), (b) gradient direction (∇**v**), and (c) vorticity direction ($\nabla\times$**v**) (see Figure 1). ϕ is defined in the inset of each plot. The solid and dashed lines identify the perpendicular and parallel orientations, respectively.

Formation of the perpendicular morphology probably favors an extended, bridging, chain conformation as depicted schematically in Figure 1. This arrangement should minimize block stretching during large-amplitude oscillatory shearing; a simplistic and possibly naïve "log-rolling" mechanism would allow the chains to accommodate the imposed strain. Extensive bridging also would account for the lack of swelling, since the

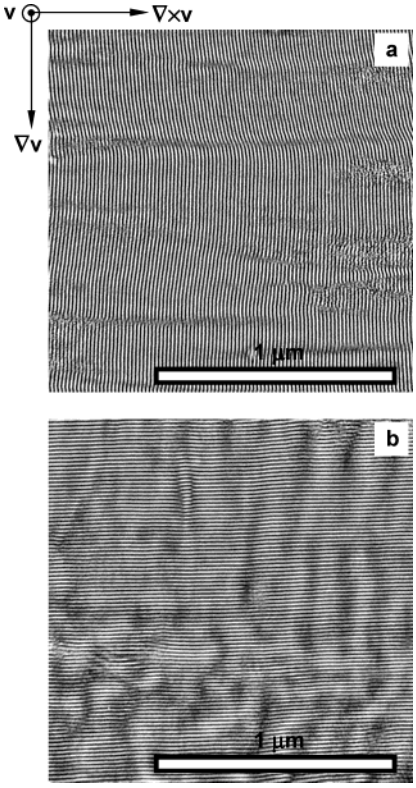

Figure 3. Representative TEM micrographs for (a) perpendicular and (b) parallel aligned SISISIS. Poly(isoprene) domains were preferentially stained with OsO_4 and appear dark in these images. The structures are viewed along the shear direction (see Figure 1).

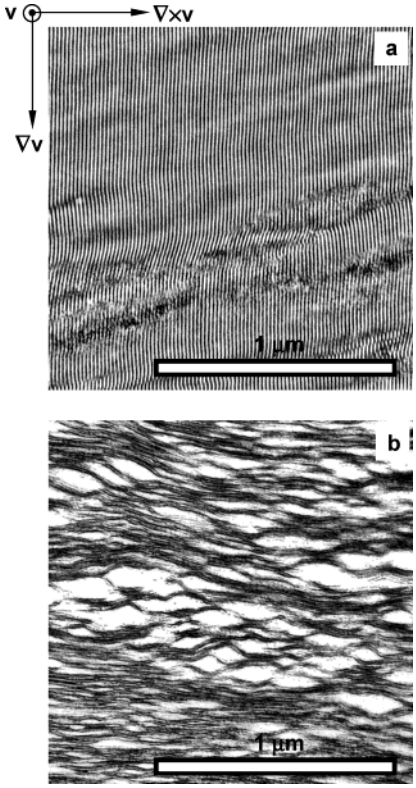

Figure 4. Representative cryo-TEM micrographs obtained after exposing thin films of (a) perpendicular and (b) parallel aligned SISISIS to tetradecane, a solvent for poly(isoprene) and a nonsolvent for poly(styrene). Poly(isoprene) domains were preferentially stained by OsO_4 and appear dark in these micrographs. The structure is viewed along the shear direction. Perpendicular lamellae were unaffected by the solvent, whereas the parallel lamellae displayed extensive buckling and delamination.

internal I blocks all would be effectively cross-linked (i.e., pinned at the glassy interface) in the presence of the selective solvent. We do not propose that all the chains adopt the fully bridged conformation indicated in Figure 1; we do, however, propose that the proportion of bridges is higher than the theoretically anticipated value (ca. 40%) for an unsheared multiblock sample.[41] Note that the equilibrium fraction of bridged and looped blocks has been the subject of considerable prior experimental and theoretical effort.[35,36,41−52] In general, the (inherently indirect) experimental results are broadly consistent with the most recent self-consistent mean-field theory calculations.[42−44]

By the same reasoning, in the parallel morphology the I blocks must be largely unconstrained, which implies predominantly looping blocks. This state of molecular conformation also would permit layer sliding, consistent with the requirements imposed by the shearing geometry. Figure 1 illustrates the most idealized molecular arrangement consistent with this concept. We suggest that the combination of low shear rate and large strain amplitude favors layer-by-layer sliding, which drives a predominantly looping conformation. Moreover, facile shearing must eliminate topological entanglements that might mechanically couple adjacent layers, thereby facilitating subsequent solvent-induced delamination. It is worth noting that a fully looped conformation is not as entropically unfavorable as it might first appear. In the unsheared sample the five internal blocks can sample bridging and looping conformations independently. If the two conformations were equally probable, then $1/2^5 = 1/32$ chains would be fully looped even before large amplitude shear was applied. For the theoretical looping probability of 0.6, almost 8% of the chains would be fully looped. Also, the small but distinct reduction in domain spacing is consistent with an increase in looping.[41,53]

These preliminary findings and our tentative interpretation suggest an important connection between shear-induced microdomain alignment and molecular conformation in linear block copolymer melts. Several previous theoretical treatments dealing with the shear alignment of lamellae have either ignored this aspect of the problem (e.g., shear-induced perpendicular order from the fluctuating disordered state[54]) or lumped elastic anisotropy into a "viscoelastic contrast" parameter without explicitly addressing the coupling between chain extension and microdomain orientation.[55] Clearly, a complete theoretical description of the effects of strain amplitude, shear rate, and segregation strength on lamellae orientation must account for block conformation. Notably, Ganesan and Fredrickson predicted an interesting response of chain conformations under shear for parallel-aligned pentablock lamellae: large strain amplitudes will drive a transformation from bridging to looping and thus generate sliding layers with predominant looping blocks.[31] This scenario is consistent with our result. Their treatment also anticipates that the spatial distribution of all-looped conformations may not be uniform, which could also be consistent with the image in Figure 4b. It is interesting to speculate on the evolution of chain conformation during flow. On the basis of linear viscoelastic measurements on this polymer in the disordered state, we may estimate a "bare" longest chain relaxation time of 0.1 s. If the primary

effect of shear is a local "melting" of the microdomains (not inconceivable, given the proximity to the ODT), then this relaxation time is much shorter than the hour time scale used to achieve macroscopic orientation. On the other hand, if the process proceeds by sequential pulling of blocks through successive domains, the relevant time scale estimated from the ordered state rheology is 0.3 s. The thermodynamic penalty for pulling one block through the other domain (especially in the initially disorganized sample) is not that large, and the entanglement restriction (about two entanglements per isoprene block) is also not prohibitive.

In summary, this communication presents a startling initial result regarding the role of chain orientation in a shear-aligned heptablock copolymer, thereby highlighting the crucial role of molecular conformation. A future publication will report on a more comprehensive set of processing conditions ($1 \leq \gamma \leq 10$ and $0.1 \leq \omega \leq 40$ rad s^{-1}) applied to SI, SIS, SISI, SISIS, SISISIS, and SISISISISIS block copolymers.

Acknowledgment. This research was supported primarily by the MRSEC program of the National Science Foundation under Award DMR-0212302.

References and Notes

(1) Keller, A.; Pedemonte, E.; Willmouth, F. M. *Nature (London)* **1970**, *225*, 538−539.
(2) Hadziioannou, G.; Mathis, A.; Skoulios, A. *Colloid Polym. Sci.* **1979**, *257*, 136−139.
(3) Koppi, K. A.; Tirrell, M.; Bates, F. S.; Almdal, K.; Colby, R. H. *J. Phys. II* **1992**, *2*, 1941−1959.
(4) Tepe, T.; Hajduk, D. A.; Hillmyer, M. A.; Weimann, P. A.; Tirrell, M.; Bates, F. S.; Almdal, K.; Mortensen, K. *J. Rheol.* **1997**, *41*, 1147−1171.
(5) Vigild, M. E.; Chu, C.; Sugiyama, M.; Chaffin, K. A.; Bates, F. S. *Macromolecules* **2001**, *34*, 951−964.
(6) Hermel, T. J.; Wu, L.; Hahn, S. F.; Lodge, T. P.; Bates, F. S. *Macromolecules* **2002**, *35*, 4685−4689.
(7) Mori, Y.; Lim, L. S.; Bates, F. S. *Macromolecules* **2003**, *36*, 9879−9888.
(8) Albalak, R. J.; Thomas, E. L. *J. Polym. Sci., Part B: Polym. Phys.* **1993**, *31*, 37−46.
(9) Riise, B. L.; Fredrickson, G. H.; Larson, R. G.; Pearson, D. S. *Macromolecules* **1995**, *28*, 7653−7659.
(10) Patel, S. S.; Larson, R. G.; Winey, K. I.; Watanabe, H. *Macromolecules* **1995**, *28*, 4313−4318.
(11) Zhang, Y.; Wiesner, U. *J. Chem. Phys.* **1995**, *103*, 4784−4793.
(12) Zhang, Y.; Wiesner, U.; Spiess, H. W. *Macromolecules* **1995**, *28*, 778−781.
(13) Zhang, Y.; Wiesner, U.; Yang, Y.; Pakula, T.; Spiess, H. W. *Macromolecules* **1996**, *29*, 5427−5431.
(14) Maring, D.; Wiesner, U. *Macromolecules* **1997**, *30*, 660−662.
(15) Leist, H.; Maring, D.; Thurn-Albrecht, T.; Wiesner, U. *J. Chem. Phys.* **1999**, *110*, 8225−8228.
(16) Kannan, R. M.; Kornfield, J. A. *Macromolecules* **1994**, *27*, 1177−1186.
(17) Gupta, V. K.; Krishnamoorti, R.; Kornfield, J. A.; Smith, S. D. *Macromolecules* **1995**, *28*, 4464−4474.
(18) Gupta, V. K.; Krishnamoorti, R.; Kornfield, J. A.; Smith, S. D. *Macromolecules* **1996**, *29*, 1359−1362.
(19) Gupta, V. K.; Krishnamoorti, R.; Chen, Z. R.; Kornfield, J. A.; Smith, S. D.; Satkowski, M.; Gothaus, J. *Macromolecules* **1996**, *29*, 875−884.
(20) Chen, Z.-R.; Kornfield, J. A.; Smith, S. D.; Grothaus, J. T.; Satkowski, M. M. *Science* **1997**, *277*, 1248−1253.
(21) Chen, Z.-R.; Issaian, A.; Kornfield, J. A.; Smith, S. D.; Grothaus, J. T.; Satkowski, M. M. *Macromolecules* **1997**, *30*, 7096−7114.
(22) Chen, Z.-R.; Kornfield, J. A. *Polymer* **1998**, *39*, 4679−4699.
(23) Larson, R. G.; Winey, K. I.; Patel, S. S.; Watanabe, H.; Bruinsma, R. *Rheol. Acta* **1993**, *32*, 245−253.
(24) Winey, K. I.; Patel, S. S.; Larson, R. G.; Watanabe, H. *Macromolecules* **1993**, *26*, 4373−4375.
(25) Winey, K. I.; Patel, S. S.; Larson, R. G.; Watanabe, H. *Macromolecules* **1993**, *26*, 2542−2549.
(26) Pinheiro, B. S.; Winey, K. I. *Macromolecules* **1998**, *31*, 4447−4456.
(27) Polis, D. L.; Smith, S. D.; Terrill, N. J.; Ryan, A. J.; Morse, D. C.; Winey, K. I. *Macromolecules* **1999**, *32*, 4668−4676.
(28) Wang, H.; Kesani, P. K.; Balsara, N. P.; Hammouda, B. *Macromolecules* **1997**, *30*, 982−992.
(29) Wang, H.; Newstein, M. C.; Krishnan, A.; Balsara, N. P.; Garetz, B. A.; Hammouda, B.; Krishnamoorti, R. *Macromolecules* **1999**, *32*, 3695−3711.
(30) Harada, T.; Bates, F. S.; Lodge, T. P. *Macromolecules* **2003**, *36*, 5440−5442.
(31) Ganesan, V.; Fredrickson, G. H. *J. Rheol.* **2001**, *45*, 161−185.
(32) Hermel, T. J.; Hahn, S. F.; Chaffin, K. A.; Gerberich, W. W.; Bates, F. S. *Macromolecules* **2003**, *36*, 2190−2193.
(33) Wu, L.; Cochran, E. W.; Lodge, T. P.; Bates, F. S. *Macromolecules* **2004**, *37*, 3360−3368.
(34) Spontak, R. J.; Smith, S. D.; Satkowski, M. M.; Ashraf, A.; Zielinski, J. M. *Stud. Polym. Sci.* **1992**, *11*, 65−88.
(35) Spontak, R. J.; Zielinski, J. M.; Lipscomb, G. G. *Macromolecules* **1992**, *25*, 6270−6276.
(36) Zielinski, J. M.; Spontak, R. J. *Macromolecules* **1992**, *25*, 653−662.
(37) Smith, S. D.; Spontak, R. J.; Satkowski, M. M.; Ashraf, A.; Lin, J. S. *Phys. Rev. B* **1993**, *47*, 14555−14558.
(38) Smith, S. D.; Spontak, R. J.; Satkowski, M. M.; Ashraf, A.; Heape, A. K.; Lin, J. S. *Polymer* **1994**, *35*, 4527−4536.
(39) Spontak, R. J.; Smith, S. D. *J. Polym. Sci., Part B: Polym. Phys.* **2001**, *39*, 947−955.
(40) Hajduk, D. A.; Ho, R.-M.; Hillmyer, M. A.; Bates, F. S.; Almdal, K. *J. Phys. Chem. B* **1998**, *102*, 1356−1363.
(41) Matsen, M. W. *J. Chem. Phys.* **1995**, *102*, 3884−3887.
(42) Watanabe, H. *Macromolecules* **1995**, *28*, 5006−5011.
(43) Watanabe, H.; Tan, H. *Macromolecules* **2004**, *37*, 5118−5122.
(44) Karatasos, K.; Anastasiadis, S. H.; Pakula, T.; Watanabe, H. *Macromolecules* **2000**, *33*, 523−541.
(45) Zhulina, E. B.; Halperin, A. *Macromolecules* **1992**, *25*, 5730−5741.
(46) Matsen, M. W.; Schick, M. *Macromolecules* **1994**, *27*, 7157−7163.
(47) Matsen, M. W.; Schick, M. *Macromolecules* **1994**, *27*, 187−192.
(48) Li, B.; Ruckenstein, E. *Macromol. Theor. Simul.* **1998**, *7*, 333−348.
(49) Matsen, M. W.; Thompson, R. B. *J. Chem. Phys.* **1999**, *111*, 7139−7146.
(50) Huh, J.; Jo, W. H.; Ten Brinke, G. *Macromolecules* **2002**, *35*, 2413−2416.
(51) Rasmussen, K. O.; Kober, E. M.; Lookman, T.; Saxena, A. *J. Polym. Sci., Part B: Polym. Phys.* **2002**, *41*, 104−111.
(52) Thompson, R. B.; Rasmussen, K. O.; Lookman, T. *J. Chem. Phys.* **2004**, *120*, 3990−3996.
(53) Lescanec, R. L.; Hajduk, D. A.; Kim, G. Y.; Gan, Y.; Yin, R.; Gruner, S. M.; Hogen-Esch, T. E.; Thomas, E. L. *Macromolecules* **1995**, *28*, 3485−3489.
(54) Cates, M. E.; Milner, S. T. *Phys. Rev. Lett.* **1989**, *62*, 1856−1859.
(55) Fredrickson, G. H. *J. Rheol.* **1994**, *38*, 1045−1067.

MA048635W